Bulletin of Engineering Geology and the Environment (2022) 81:474
https://doi.org/10.1007/s10064-022-02969-5

ORIGINAL PAPER

Model test of a geogrid-reinforced tailing accumulation dam

Changbo Du[1] · Ben Niu[1] · Fu Yi[2] · Lidong Liang[1]

Received: 28 March 2022 / Accepted: 2 October 2022

Abstract
This study aimed to explore the retardation characteristics of different geogrid-reinforced layers and mesh sizes in the failure process of a reinforced tailings dam. The Qidashan tailings of Ansteel Mining were considered as the engineering background. The tailings-dam model test was conducted by laying a geogrid in the tailings dam. We analyzed the effects of different reinforcement layers and mesh sizes of reinforced tailings dams on the surface settlements, phreatic lines, and vertical pressures within the dam body. We explored and tested the reinforcement mechanism and its effect. The test results indicate that the final surface settlement yields a positive correlation with an increase in the number of reinforced layers. The surface settlement increases rapidly at first before becoming stable as the geogrid mesh size decreases. The phreatic line of the dam body can be reduced considerably by increasing the number of reinforcement layers. Moreover, a reasonable mesh size of the reinforcement can reduce the phreatic line of the dam body. The vertical pressure inside the dam decreases considerably as the number of reinforced layers increases. With a smaller geogrid mesh size, vertical pressure inside the dam body decreases. Therefore, reinforcement has a significant retarding effect on the development of tailing accumulation dam failure and enhances its stability.

Keywords Model test · Reinforcement of the tailings dam · Geogrid · Phreatic line

Introduction

Tailing ponds are an important facility for the production of mining enterprises. Their operation statuses are related to the smooth progress of mine production and construction, as well as people's safety and property downstream of the dam and surrounding environment (Mcdermott and Sibley 2000; Marcus et al. 2001; Fourie et al. 2001; Kemper and Sommer 2002; Tynybekov and Aliev 2007; Zhuang et al. 2022). Reinforcement methods have been comprehensively studied and applied in many fields (Zhao et al. 2020; Chen and Yu 2009). Therefore, some scholars have also studied the application of reinforcement methods for improving the stability of the tailings dams. Yi and Du (2020) studied the influence of geogrid and geotextile reinforcements on the stability of the tailing accumulation dams, revealing that the quasi-cohesive force of reinforced tailings increases linearly as a function of the number of reinforced layers. Zheng et al. (2019) used basalt to reinforce tailings dams and showed that the mechanical properties of basalt fiber-reinforced tailings increase as a function of fiber length and content. Liu et al. (2021a) also studied basalt fiber-reinforced tailings and revealed that adding basalt fibers into tailings can enhance the shear strength and cohesion of tailings. Liu et al. (2021b) studied the influence of reinforcement on a tailings dam at an overtopping dam break and demonstrated that reinforcement has an effective blocking effect on the movement of tailing particles.

As prototype research is difficult to achieve, it is necessary to introduce a physical model for experimental research. As an important means of engineering scientific research, physical models have been extensively used in many fields (Hancock 2004; Chen et al. 2015; Shen et al. 2012; Bathurst and Ezzein 2016; Festugato et al. 2015; Wei et al. 2009; Consoli et al. 2017; Du and Yi 2020). Although a physical phenomenon cannot be described completely using a

✉ Ben Niu
niu18535527973@163.com

✉ Fu Yi
yifu9716@163.com

[1] School of Civil Engineering, Liaoning Technical University, Fuxin, Liaoning Province 123000, China

[2] College of Architecture and Transportation, Liaoning Technical University, Fuxin, Liaoning Province 123000, China

Published online: 15 October 2022

physical model, it can be observed qualitatively. Using the similarity between the model and prototype, the laws and mechanisms of the physical phenomena can be analyzed, and quantitative analysis can be conducted through the scale bar to a certain extent. Recently, scholars have conducted considerable work on the model testing of reinforced structures. Dash et al. (2004) compared the results obtained from laboratory model tests of the bearing capacity of a sand bed reinforced with randomly distributed geogrid elements on a geocell, plane geogrid, or strip foundation and found that geocell reinforcement was the most favorable reinforcement form. Yin et al. (2005) used the tailings in the Longdu tailing pond as the test material. They considered the Longdu tailing pond as the prototype stacked tailings dam model and then conducted a failure model test of the reinforcement of the tailings dam. In particular, the failure model test of the reinforced tailings dam was conducted, and the reinforcement effect of the tailings dam with tailing accumulation was tested. Subsequently, different failure modes and mechanisms of reinforced and unreinforced tailings dams were obtained. Matsuoka and Liu (2003) proposed a new geotextile bag reinforcement technology for slopes and foundations and studied the enhancement mechanism, engineering characteristics, and design methods. Mehrjardi and Khazaei (2017) considered the size effects of fill particles, geogrid aperture, and loading plate on reinforced soil-retaining walls. Moreover, they evaluated the response of the retaining wall model by the applied load and surface settlement to understand the characteristics of the retaining wall of the reinforced soil. Ehrlich et al. (2012) studied the effect of compaction on the performance of geogrid-reinforced earth walls and revealed that compaction plays a decisive role in terms of the reinforcement tensions and post-construction displacements. Portelinha and Zornberg (2017) studied the influence of the permeability of fill on the structural performance of retaining walls. A full-scale retaining wall with reinforced soil was established, and an irrigation system was used to simulate the rainfall process. The changes in the filling volume's moisture content, matrix suction, wall displacement, and geogrid strain were measured. Jing et al. (2019) conducted an overtopping failure model test of a reinforced tailings dam and demonstrated the blocking effect of the reinforcement belt in the overtopping failure process of the tailings dam. They concluded that considering reinforcement measures can effectively reduce the overtopping failure of tailing pond floods.

Based on the design data of Ansteel's Qidashan iron ore tailing pond, geogrids were laid in the tailings dam, and model tests of reinforced tailing accumulation dams with a different number of reinforced layers and different geogrid mesh sizes were conducted. They revealed the effects of the retardation characteristics of the different numbers of geogrid reinforcement layers and mesh sizes on the damage process of the dam body, stability of the geogrid-reinforced tailing accumulation dam and possible damage, and reinforcement effect after the dam body became the reinforced mechanism.

Model test device and material

Engineering background and similarity scales

We considered the main dam of the Fengshuigou tailing pond in the Qidashan concentrator of Ansteel Mining as an example. The tailing pond accumulation dam adopts the upstream flushing and filling method and multipipe scattered ore draws. The height of each sub-dam of the tailing accumulation dam was approximately 5 m, the average outer slope ratio of the accumulation dam was approximately 1:5, the total storage capacity was approximately 6.84×10^8 m^3, and the tailing pond was first-order. This model test simulates the main dam of the Qidashan tailing pond with a maximum dam height of 120 m, which is reduced with a scale of 1:300. In this model, there is a 30-m accumulation layer at the bottom of the dam, considered as part of the accumulation dam in the model. Therefore, the vertical dimension of the model is 0.5 m. The primary dam height was 20 m, and the external slope ratio was 1:2. This study did not consider the influence of the main dam on the stability of the accumulation dam. Therefore, the primary dam was not built during the model-stacking process. Considering that the model test of the reinforced tailings dam is to reveal the retardation characteristics of different geogrid-reinforced layers and mesh sizes on the dam failure process, the model test results are analyzed according to the single-factor method. In this experiment, the outer slope ratio of the model was 1:2, and the inner slope ratio was fixed at 1:5, as shown in Fig. 1. Other similarity scales evaluated in this study are listed in Table 1 (Jing et al. 2011).

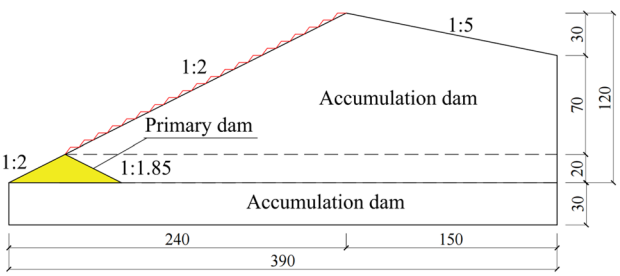

Fig. 1 Section sizes of the main dam of the Fengshuigou tailing pond (unit: m)

Table 1 Similarities between physical model and prototype

Similarity ratio	Displacement	Length	Area	Volume	Gravitational acceleration	Gravity	Porosity	Permeability coefficient	Flow	Time/ seepage
Prototype	λ	λ	λ^2	λ^3	1	1	1	1	$\lambda^{5/2}$	λ^2
Model	1	1	1	1	1	1	1	1	1	1

λ is the proportional coefficient

Test device

The test device consists of a model box, vertical loading system, and data acquisition system, as shown in Fig. 2. The size of the model box was 1320 mm × 800 mm × 700 mm (length × width × height). To observe the evolution process of the phreatic line of the tailing accumulation dam, a transparent tempered glass with a thickness of 12 mm was pasted on the frame of the model box and sealed to prevent the water in the dam body from draining through the gap in the model box. Glass plates were not pasted on the wall of the modeled accumulation dam in the drainage direction, which facilitated the timely discharge of the water precipitated from the accumulation dam and reduced the impact of accumulated water. The loading system adopted an integrated design using a 1:2 ratio lever to apply an overlying pressure. Additionally, there was a pressure plate under the lever node to ensure the uniform application of the overlying pressure. The overlying pressure was applied by adding suitable weights to the load tray. The data acquisition system consists of a transparent acrylic tube, dial indicator, and micro-pressure gauge used to measure the phreatic line, surface settlement, and vertical pressure inside the dam, respectively. The specific instrument layout is shown below.

Layout of measuring instruments

The layout of the measurement instruments used in the experiment is shown in Fig. 3. Three main measurement instruments were used for the model test:

1 The dial indicator was arranged above the dam body and placed horizontally on the bearing plate to measure the surface settlement of the dam body during the test (see Fig. 2).
2 Four acrylic pipes were arranged at the boundary of the model box to observe the development of the dam's water level and phreatic line during the test (see Fig. 2).
3 Ten miniature earth pressure gauges were arranged inside the dam body, as shown in Fig. 3, to measure the pressure change inside the dam body during the test.

The miniature earth pressure gauge uses the LY-350 strain type (see Fig. 4a) with a small volume and waterproof function. The main technical indicators are listed in Table 2. This strain type is suitable for model tests on a small scale. The data acquisition instrument used in the test is a DH3817K dynamic and static strain gauge (Fig. 4b). The measurement type of the micro-pressure gauge in this test is the

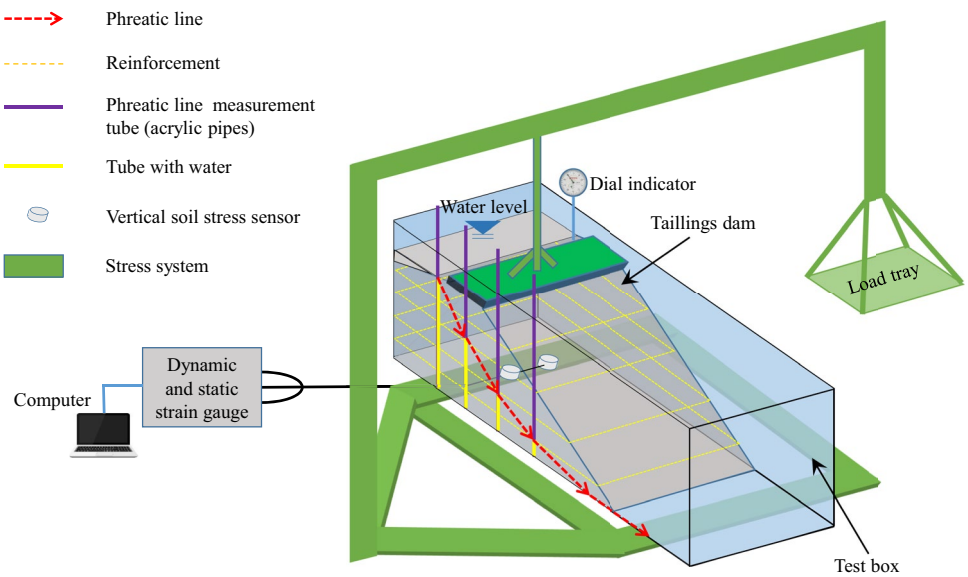

Fig. 2 Dimensions of the test device

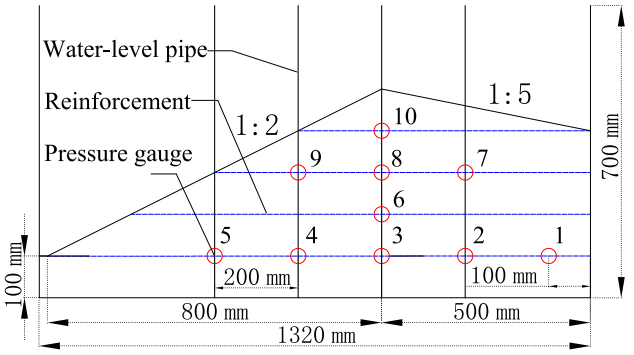

Fig. 3 Schematic of the layout of test instruments

compressive strain inside the dam. The micro earth pressure gauge is connected to the data acquisition instrument, and the full-bridge wiring mode is selected.

Selection of model test materials

This study introduces a physical model to conduct a similarity test research. The study uses the similarity between the model and prototype to analyze the laws and mechanisms of the physical phenomena and make qualitative conclusions on the research object. Therefore, the test materials discussed in this paper are from Ansteel's Qidashan iron ore tailing pond. Scholars (Jing et al. 2019; Yin et al. 2005) also used prototype sand to conduct similar model tests and reached credible conclusions. The tailing filler used in the test was obtained from the Fengshuigou tailing pond of the Qidashan concentrator of Ansteel Mining, with a density of 1.83 g/cm^3 and a moisture content of 3.75%. The physical properties of the tailings are as follows: effective particle size $d_{10}=0.10$ mm, median particle size $d_{30}=0.19$ mm, and restricted particle size $d_{60}=0.30$ mm. After calculations, the nonuniformity coefficient $C_u=3<5$ and curvature coefficient $C_c=1.2$ had values in the range of 1–3, thus indicating that the tailings were poorly graded; the particle grading curve is shown in Fig. 5. The mechanical indicators of the tailings are the natural bulk density $\gamma=18$ kN/m^3, cohesion $c=9.4$ kPa, friction angle $\varphi=28°$, Poisson ratio $v=0.42$, elastic modulus $E=1.6\times10^5$ kPa, and permeability coefficient $K=2.75\times10^{-4}$ cm/s.

Table 2 Performance index of the miniature earth pressure gauge

Type	LY-350
Measuring range/MPa	0–100
Resolution/% full scale (F·S)	≤0.05
Dimensions/mm	28×10 (diameter×height)
Impedance/Ω	350
Insulation resistance/MΩ	≥200

The reinforcement used in this model test was an EGA30 geogrid, which was cut into different mesh sizes. The EGA30 geogrid has been applied in various reinforcement engineering environments, and good results were obtained. Table 3 summarizes the specific material performance parameters.

Test scheme and steps

According to the test conducted by Du et al. (2022), when studying a reasonable mesh size of the geogrid-reinforced tailings, the geogrid is into different mesh sizes, and the original dimensions are 12.7 mm×12.7 mm (C). The geogrid is then cut to dimensions equal to 25.4 mm×25.4 mm (B) and 38.1×38.1 mm (A) (see Fig. 6).

Before the formal test, we conducted a series of pretests. Finally, the overburden pressure of the dam body was set to 1 kN, which can make the compaction state of the accumulation dam similar to the actual compaction of the tailings dam onsite. According to the pretest results, the water addition

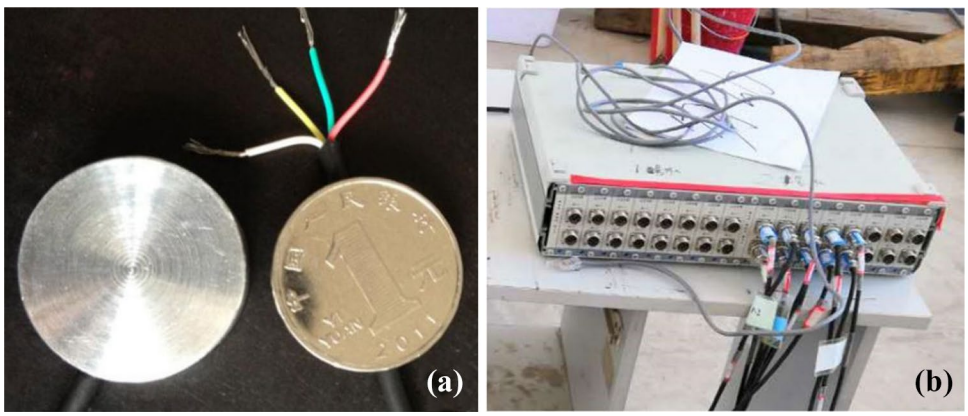

Fig. 4 Instrument photographs. **a** Miniature earth pressure gauge (LY-350 strain type) and **b** DH3817K dynamic and static strain gauge device

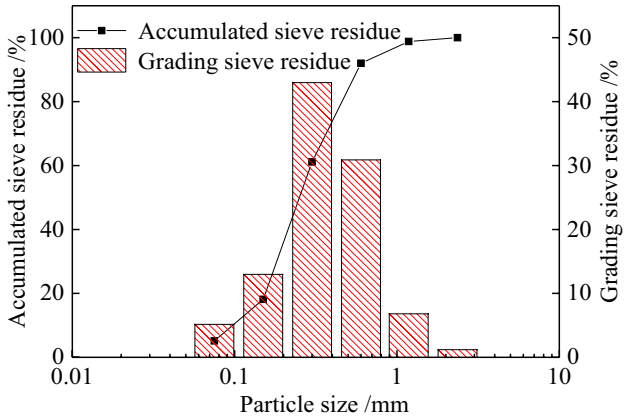

Fig. 5 Gradation curve of the tailing sand

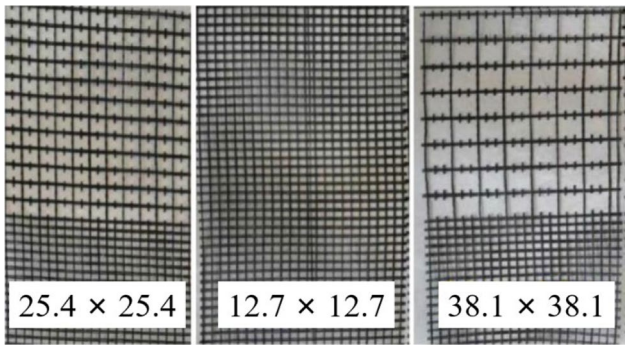

Fig. 6 Geogrids with different mesh sizes

to the dam body was set to 40 L, which can make the accumulation dam meet the phreatic line state of the real tailing pond (see Fig. 7).

There are six groups of simulation test schemes for geogrid-reinforced tailings. The influence of the number of reinforced layers and mesh sizes of the geogrid on the surface settlement, internal pressure, and phreatic line of the reinforced tailing accumulation dam were analyzed. The specific test design scheme is shown in Table 4. The reinforcement positions of the geogrid with different reinforced layers are shown in Fig. 8.

The steps of testing the geogrid-reinforced tailings dam model were as follows:

1 The amount of tailing sand used for each test was made consistent. The tailings of the dam were stacked in layers and compacted, and then they were paved. The geogrid was laid according to the requirements of different test schemes, and the laying structure of the geogrid was positioned such that the outer side was folded back; additionally, the micro earth pressure gauge was arranged as shown in Fig. 3 during the stacking process.
2 After model stacking, the model was maintained for 2 h. The overlying pressure was applied above the accumulation dam through a lever, and a large-range dial indicator was arranged above the dam body before starting the test.
3 After the test started, water was slowly injected into the dry beach surface of the dam body until the required water injection volume was reached. The variation law of the internal pressure against time was observed by connecting the computer with the data acquisition instrument, with the surface settlement of the dam crest in different periods recorded simultaneously.
4 The surface settlement of the dam crest and vertical pressure inside the dam was observed to be stable, and the test was terminated.
5 Subsequently, the model was disassembled. During the disassembling process, samples were obtained according to the position of the micro earth pressure gauge in Fig. 3, and the drying oven was then used to measure the water content of these 10 sampling positions.
6 After disassembling the test model, test results were analyzed. Figure 9 shows the results after model stacking.

Table 3 Technological parameters of the geogrid

EGA30 geogrid		Technical index
Mesh size (length × width)/mm		12.7 × 12.7
Fracture strength/(kN■m^{-1})	Radial	30
	Zonal	30
Elongation at break ≥ /%	Radial	4
	Zonal	4
Temperature resistance ≥ /℃		− 100–280

Test results and analysis

Influences of the reinforced layers

Settlement analysis of the dam crest

Figure 10a shows the temporal variation in the dam surface settlement in different reinforced layers, where the variation of the surface settlement with time was approximately the same. The surface settlement increased almost linearly with time, and the surface settlement of the dam tended to be stable at approximately 80 min. When four-reinforced layers were used, the variation range was the largest, and the final surface settlement was 18.3 mm. In the cases where 1, 2, and 4 reinforced layers were used, the final surface settlement increased by 61.4%, 77.1%, and 161.4%, respectively. In particular, the variation range of the surface settlement increased when the number of reinforced

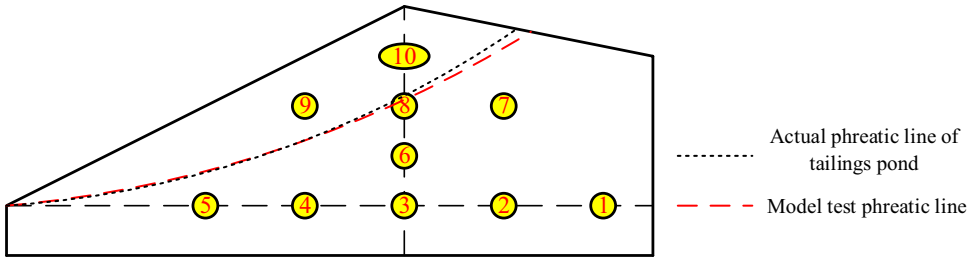

Fig. 7 Comparison between the model test and actual phreatic lines following the addition of 40 L of water

layers increased. By fitting the final surface settlement of the dam crest with the reinforced layers, as shown in Fig. 10b, the final surface settlement is considered positively correlated with the number of reinforced layers, thus meeting the linear relationship $y = 7.54 + 2.69x$. Therefore, the number of reinforced layers has a significant impact on the surface settlement of the dam. This result shows that increasing the reinforced layers of the accumulation dam can considerably improve the bearing capacity of the dam body and enhance its overall compactness because, after the phreatic line maintains a high water level for a certain period, the meshing effect of the geogrid reduces the tailing sand downfall of the dam body, thus resulting in a smaller displacement change in the vertical direction, which increases the deformation resistance and stability of the dam body.

Phreatic line analysis in the tailings dam

After the test, 10 micro earth pressure gauge positions embedded in the modeled box dam body were sampled to measure the moisture contents of the tailings at these positions in combination with the water-level results measured by the four water-level pipes arranged at the boundary of the model. The variation of the accumulation dam's phreatic line at different reinforced layers was obtained as shown in Fig. 11. Compared with the unreinforced dam, the phreatic line of the tailing accumulation dam decreased, especially for the inner slope of the dam. Based on the premise that the reinforcement spacing remained unchanged, an overall decrease of the phreatic line of the dam body became evident as the reinforced layers of the accumulation dam increased. In particular, the increase in the reinforced layers can significantly reduce the phreatic line of the dam body, thus indicating that the reinforcement of the tailing accumulation dam can promote the discharge of water and reduce the phreatic line in the dam body. This is because the reinforcement of the tailings dam can make the reinforced tailing complex form a drainage prism that can promote the drainage of water inside the dam and reduce the phreatic line inside the dam.

Internal pressure analysis of the tailings dam

During the test, pressure changes at 10 micro-pressure gauge positions inside the dam body (see Fig. 3) were measured. The pressures at 10 positions were divided into horizontal (positions 1, 2, 3, 4, and 5) and vertical (positions 3, 6, 8, and 10) positions. The variations of the vertical pressure at different positions inside the tailing accumulation dam, which comprised different reinforced layers, are shown in Fig. 12. The maximum vertical pressure in both the horizontal and vertical directions is at position 3, that is, the position with the lowest pressurization of the dam body. The maximum vertical pressures of the one-, two-, and four-reinforced layer cases were 18.6%, 22.3%, and 39.9% lower than that of the unreinforced layer, respectively. When the

Table 4 Model test scheme

Test group	Reinforced layers	Outer slope ratio	Geogrid mesh size	Remarks
1	0	1:2	No reinforcement	Reference model test of the plain tailing accumulation dam
2	1		Geogrid B	Combined with test 1, the influence of reinforced layers on the model test is analyzed
3	2			
4	4			
5	2		Geogrid A	Combined with tests 1 and 3, the influence of the geogrid mesh size on the model test is analyzed
6			Geogrid C	

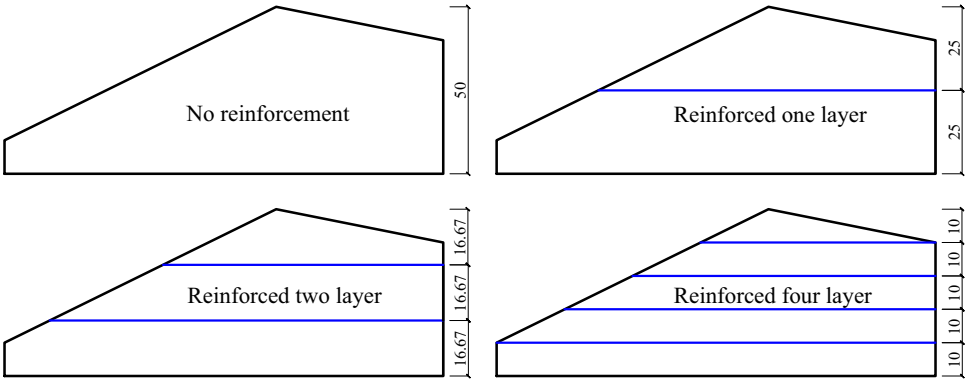

Fig. 8 Schematic of the geogrid layout (unit: cm)

reinforcement spacing remains unchanged, the decrease in the vertical pressure in the dam body becomes evident when the number of the reinforced layers of the tailing accumulation dam increases, thus indicating that the reinforcement of the accumulation dam can reduce the vertical pressure in the dam body and enhance its stability. Owing to the fact that the laying structure of the geogrid causes the outer side to be folded back, the geogrid forms a net pocket that can convert the vertical pressure inside the dam body into a horizontal tension that the geogrid can bear. Subject to the blocking effect of the geogrid, the tailings do not fall to reduce the internal pressure of the dam body, thus resulting in a smaller change rate of the internal stress of the reinforced tailings dam body than that of the plain tailings dam.

Influences of the geogrid mesh size

Settlement analysis of the dam crest

The variation in the surface settlement of the tailings dam with time at different geogrid mesh sizes is shown in Fig. 13a. When unreinforced, the final surface settlement is 7.0 mm.

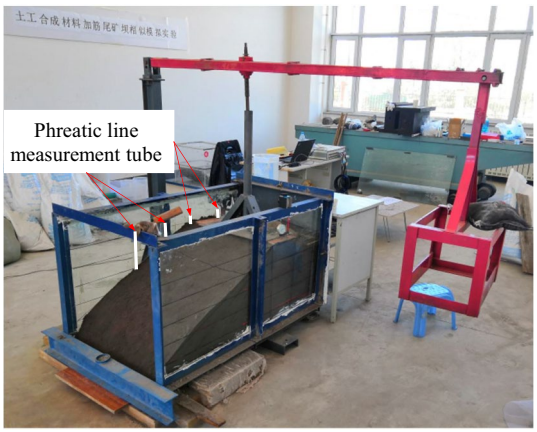

Fig. 9 Test device

When the geogrid mesh sizes are A, B, and C, the final surface settlements are 9.2 mm, 12.4 mm, and 12.3 mm, respectively, meaning, when the geogrid mesh sizes are A, B, and C, the final surface settlement increases by 31.4%, 77.1%, and 75.7%, respectively, compared with that without reinforcement. The final surface settlement first increases rapidly and then stabilizes with a decrease in the geogrid mesh size, thus indicating that the geogrid mesh size has a certain impact on the dam surface settlement (see Fig. 13b). When the mesh size is reduced from A to B, the net pocket effect provided by the geogrid is gradually enhanced and leads to the increase of the dam crest surface settlement. When the mesh size is reduced from B to C, the mesh pocket effect caused by the geogrid continues to increase. However, because the drainage channels provided by the geogrid with two mesh sizes can rapidly discharge the water in the dam body, the settlements of the dam crest surfaces are similar.

Phreatic line analysis in the tailings dam

The variation in the phreatic line of the tailings dam reinforced with different geogrid mesh sizes is shown in Fig. 14. The geogrid mesh size has a certain impact on the phreatic line inside the dam in that a reasonable geogrid mesh size can effectively reduce the phreatic line of the dam. The influence of the reinforcement on the phreatic line is caused by the drainage channel provided by the reinforcement, and the mesh sizes that are significantly small or large are not conducive to the water discharge in the dam body. When the mesh size of the geogrid is A, the drainage channels provided are too few to achieve the best drainage effect.

Internal pressure analysis of the tailings dam

The variation relationship of the vertical pressure at different positions in the tailings dam at different geogrid mesh sizes is shown in Fig. 15. As the mesh size of the geogrid decreases, the vertical pressure inside the dam decreases. When the geogrid mesh sizes are A, B, and C, the maximum

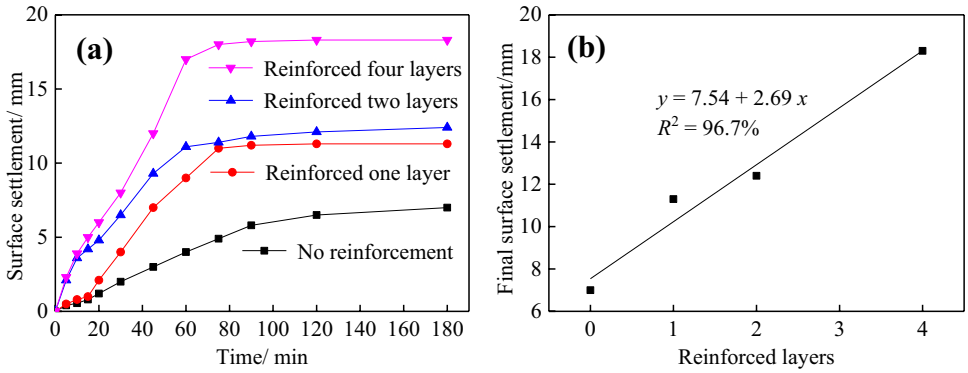

Fig. 10 Temporal variations of dam crest surface settlement at different geogrid layers. **a** Surface settlement and time. **b** Final surface settlement as a function of the reinforced layers

vertical pressure is reduced by 4.7%, 22.3%, and 28.5%, respectively, compared with that without reinforcement. When the reinforcement spacing remains unchanged, the vertical pressure inside the dam decreases gradually with a decrease in the geogrid mesh size. However, when the mesh size of the geogrid is reduced, the effect of reducing the vertical pressure inside the dam begins to weaken. As part of the vertical pressure is transformed into the horizontal tension acting on the geogrid by the mesh pocket effect, the reduction of the mesh size leads to the increase of the transformed vertical pressure, thus resulting in the gradual weakening of the vertical pressure inside the dam as the mesh size of the reinforcement decreases.

Discussion

By conducting model tests on the reinforced tailing accumulation dam with different reinforcement layers and geogrid mesh sizes, the retardation characteristics of different geogrid reinforcement layers and mesh sizes on the failure process of the dam were observed. This study provides an effective method for exploring the effects of a reasonable number of reinforced layers and mesh size range for geogrid-reinforced tailings.

Based on the test results, the effects of different reinforced layers and geogrid mesh sizes on the settlement of the top of the dam body, as well as the internal phreatic line and pressure, were analyzed. The geogrid provided a drainage channel for the reinforced tailing accumulation dam. As the reinforcement layers increase, more drainage channels are added, and a lower phreatic line larger range of settlement variation at the top of the dam body and lower internal pressure of the dam body are achieved. When the number of reinforced layers was less than four, the overall performance of the dam body increased as a function of the number of reinforced layers. The different mesh sizes of the geogrid also affected the drainage effect of the drainage channel and blocking characteristics during dam failure. This study determined a reasonable mesh size with dimensions of approximately 25.4 mm × 25.4 mm (B). In an article published by Du et al. (2022), the reported desired geogrid-reinforced tailing mesh size range is similar to that reported in this study. Therefore, the mesh size range of the geogrid-reinforced tailings is accurate, and the mesh size within this range can optimize the friction strength of the geogrid–tailing interface, help increase the settlement of the top of the dam body, and reduce the phreatic line and pressure inside the dam body, thus improving the stability of the dam body.

Owing to the test conditions, the number of selected reinforced layers shall not exceed four. Additional control experiments should be conducted to determine whether the overall performance of the dam body increases as the number of reinforced layers increases. The geogrid selected in this study, which is a two-way geogrid, and the application of other types of geogrids and geocells should be studied further.

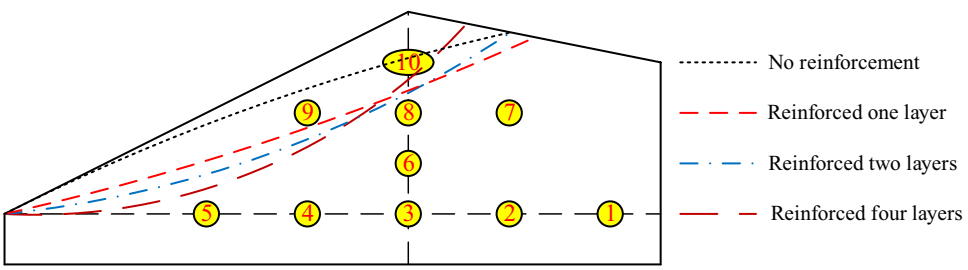

Fig. 11 Variation of phreatic lines of a tailings dam at different geogrid layers

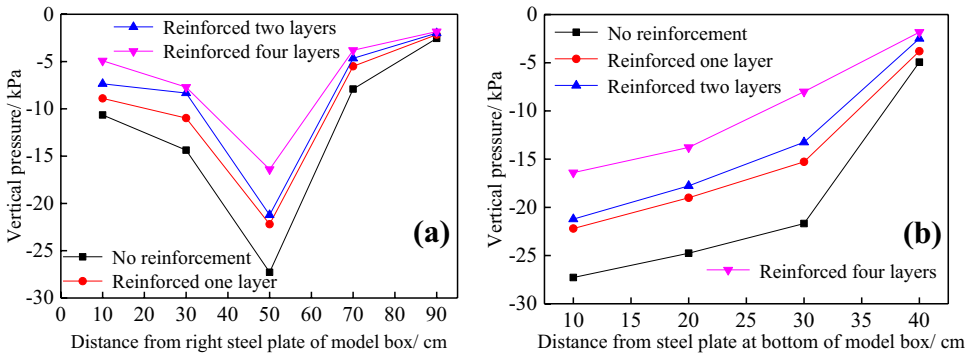

Fig. 12 Variation of vertical pressure in dams at different geogrid layers. **a** Horizontal and **b** vertical directions

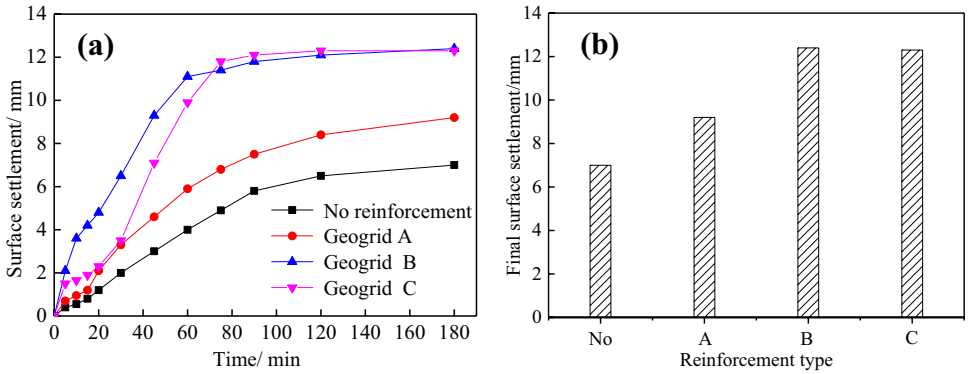

Fig. 13 Variations of surface settlements of the dam crest at different geogrid mesh sizes. **a** Temporal variations of surface settlements and **b** final surface settlement and different geogrid mesh sizes

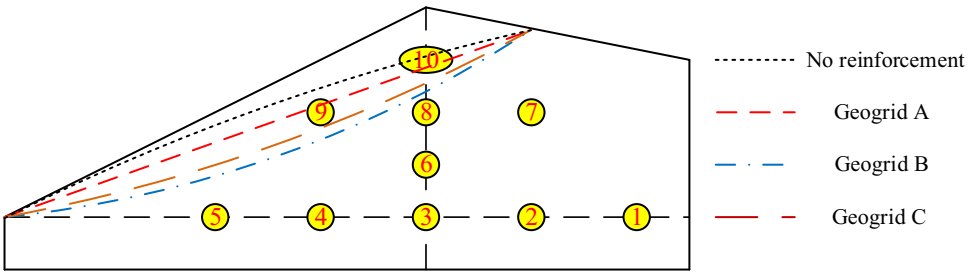

Fig. 14 Variations of the phreatic lines of the tailings dam at different geogrid mesh sizes

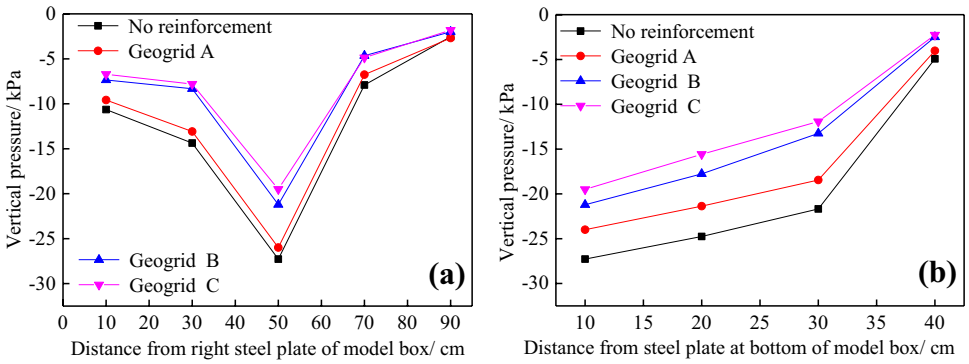

Fig. 15 Variations of vertical pressure in dams at different geogrid mesh sizes. **a** Horizontal and **b** vertical directions

Conclusions

The geogrid improves the stability of the tailings dam body, significantly improves the mechanical properties of the dam body, and decelerates the failure process of the dam body. Furthermore, the number of reinforcement layers and mesh size influences the retardation characteristics of the geogrid on the tailing accumulation dam. The main conclusions are as follows:

1 Reinforcement can significantly improve the ultimate bearing capacity of the tailing accumulation dam. There was a linear positive correlation between the final surface settlement and number of reinforced layers. The final surface settlement first increased rapidly and then stabilized when the geogrid mesh size decreased.
2 Reinforcement can promote water discharge inside the tailing accumulation dam. Increased reinforced layers and reasonable geogrid mesh size can significantly reduce the phreatic lines of the dam body and dam, respectively.
3 Reinforcement can reduce the vertical pressure inside the tailing accumulation dam body and enhance the stability of the dam body. With an increase in the number of reinforced layers, the vertical pressure inside the dam decreases significantly. A reasonable geogrid mesh size can reduce the vertical pressure inside the dam.

Acknowledgements We appreciate the editor and anonymous reviewers' for their useful comments.

Author contribution Conceptualization, Changbo Du; methodology, Changbo Du; formal analysis and investigation, Ben Niu; writing — original draft preparation, Ben Niu and Lidong Liang; writing — review and editing, Changbo Du; supervision, Fu Yi. All authors have read and agreed to the published version of the manuscript.

Funding This research was funded by the National Natural Science Foundation of China (51774163) and the youth fund of Liaoning Provincial Department of Education (LJKQZ2021153) and the discipline innovation team of Liaoning Technical University (LNTU20TD-12). We appreciate the editor and anonymous reviewers' for their useful comments.

Data availability Not applicable.

Declarations

Conflict of interest The authors declare no competing interests.

References

Bathurst RJ, Ezzein FM (2016) Geogrid pullout load-strain behaviour and modelling using a transparent granular soil. Geosynth Int 23(4):271–286. https://doi.org/10.1680/jgein.15.00051

Chen JF, Yu SB (2009) Centrifuge modeling of a geogrid-reinforced embankment with lime-stabilized soil as backfill on soft soil. Bull Eng Geol Env 68(4):511–516. https://doi.org/10.1007/s10064-009-0231-0

Chen SC, Feng ZY, Wang CA, Hsu TY (2015) A large-scaletest on overtopping failure of tow artificial dams in Taiwan. Eng Geol Soc Territory 2:1177–1181. https://doi.org/10.1007/978-3-319-09057-3_206

Consoli NC, Nierwinski HP, Da Silva AP, Sosnoski J (2017) Durability and strength of fiber-reinforced compacted gold tailings-cement blends. Geotext Geomembr 45(2):98–102. https://doi.org/10.1016/j.geotexmem.2017.01.001

Dash SK, Rajagopal K, Krishnaswamy NR (2004) Performance of different geosynthetic reinforcement materials in sand foundations. Geosynth Int 11(1):35–42. https://doi.org/10.1680/gein.2004.11.1.35

Du CB, Niu B, Wang L, Yi F, Liang LD (2022) Experimental study of reasonable mesh size of geogrid reinforced tailings. Sci Rep 12(1):1–9. https://doi.org/10.1038/s41598-022-13980-x

Du CB, Yi F (2020) Analysis of the elastic-plastic theoretical model of the pull-out interface between geosynthetics and tailings. Adv Civil Eng 8:1–22. https://doi.org/10.1155/2020/5680521

Ehrlich M, Mirmoradi SH, Saramago RP (2012) Evaluation of the effect of compaction on the behavior of geosynthetic-reinforced soil walls. Geotext Geomembr 34:108–115. https://doi.org/10.1016/j.geotexmem.2012.05.005

Festugato L, Consoli NC, Fourie A (2015) Cyclic shear behaviour of fibre-reinforced mine tailings. Geosynth Int 22(2):196–206. https://doi.org/10.1680/gein.15.00005

Fourie AB, Blight GE, Papageorgiou G (2001) Static liquefaction as a possible explanation for themerrie spruit tailings dam failure. Can Geotech J 38(4):707–719. https://doi.org/10.1139/t00-112

Hancock GR (2004) The use of landscape evolution models in mining rehabilitation design. Environ Geol 46(5):561–573. https://doi.org/10.1007/s00254-004-1030-3

Jing XF, Chen YL, Williams DJ, Serna ML, Zheng H (2019) Overtopping failure of a reinforced tailings dam: laboratory investigation and forecasting model of dam failure. Water 11(2):315. https://doi.org/10.3390/w11020315

Jing XF, Yin GZ, Wei ZA, Li XS, Wang ML (2011) Model experimental study of collapse mechanism and broken mode of tailings dam. Rock Soil Mech 32(05): 1377–1384+1404. https://doi.org/10.16285/j.rsm.2011.05.039

Kemper T, Sommer S (2002) Estimate of heavy metal contamination in soils after a mining accident using reflectance spectroscopy. Environ Sci Technol 36(12):2742–2747. https://doi.org/10.1021/es015747j

Liu JZ, Yang H, Zhang DM, Wang Y, Xiao WJ, Ye C et al (2021a) Mechanical and permeation response characteristics of basalt fibre reinforced tailings to different reinforcement technologies: an experimental study. Royal Soc Open Sci 8(9):210669. https://doi.org/10.1098/rsos.210669

Liu K, Cai H, Jing XF, Chen YL, Li L, Wu SW et al (2021b) Study on hydraulic incipient motion model of reinforced tailings. Water 13(15):2033. https://doi.org/10.3390/w13152033

Marcus WA, Meyer GA, Nimmo DWR (2001) Geomorphic control of persistent mine impacts in a Yellowstone Park stream and implications for the recovery of fluvial systems. Geology 29(4):355–358. https://doi.org/10.1130/0091-7613(2001)029%3c0355:GCOPMI%3e2.0.CO;2

Matsuoka H, Liu SH (2003) New earth reinforcement method by geotextile bag. Soils Found 43(6):173–188. https://doi.org/10.3208/sandf.43.6_173

Mcdermott RK, Sibley JM (2000) The aznalcollar tailings dam accident-a case study. Miner Resour Eng 9(1):101–118. https://doi.org/10.1142/S0950609800000111

Mehrjardi GT, Khazaei M (2017) Scale effect on the behaviour of geogrid-reinforced soil under repeated loads. Geotext Geomembr 45(6):603–615. https://doi.org/10.1016/j.geotexmem.2017.08.002

Portelinha FHM, Zornberg JG (2017) Effect of infiltration on the performance of an unsaturated geotextile-reinforced soil wall. Geotext Geomembr 45(3):211–226. https://doi.org/10.1016/j.geotexmem.2017.02.002

She LY, Zhou KP, Wei ZA, Chen YL (2012) Research on geosynthetics in tailings dam reinforcement. Adv Mater Res 402:675–679. https://doi.org/10.4028/www.scientific.net/AMR.402.675

Tynybekov AK, Aliev MS (2007) The ecological condition of Kadji-Sai uranium tailings. Environ Secur Pub Safe 191–195. https://doi.org/10.1007/978-1-4020-5644-4_16

Wei ZA, Yin GZ, Li GZ, Wang JG, Wan L, Shen L (2009) Reinforced terraced fields method for fine tailings disposal. Miner Eng 22(12):1053–1059. https://doi.org/10.1016/j.mineng.2009.03.014

Yi F, Du CB (2020) Triaxial testing of geosynthetics reinforced tailings with different reinforced layers. Materials 13(8):1943. https://doi.org/10.3390/ma13081943

Yin GZ, Wei ZA, Wan L, Zhang DM (2005) Test study on stability of fine grained tailings dam in geo-grid reinforcement situation. Chinese J Rock Mech Eng (6):1030–1034. (in Chinese) https://doi.org/10.3321/j.issn:1000-6915.2005.06.023

Zhao RF, Zhang SN, He J, Gao W, Jin D, Xie LQ (2020) Experimental study on freezing and thawing deformation of geogrid-reinforced silty clay structure. Bull Eng Geol Env 79(6):2883–2892. https://doi.org/10.1007/s10064-020-01725-x

Zheng BB, Zhang DM, Liu WS, Yang YH, Yang H (2019) Use of basalt fiber-reinforced tailings for improving the stability of tailings dam. Materials 12(8):1306. https://doi.org/10.3390/ma12081306

Zhuang Y, Jin KP, Cheng QG, Xing AG, Luo H (2022) Experimental and numerical investigations of a catastrophic tailings dam break in Daye, Hubei, China. Bull Eng Geol Env 81(9):1–16. https://doi.org/10.1007/s10064-021-02491-0